

Supporting information

Responsive spiral photonic structures for visible vapor sensing, pattern transformation and encryption

Jing Qian¹, Srikanth Kolagatla², Aleksejus Pacalovas,² Xia Zhang¹, Larisa Florea^{2*}, A. Louise
Bradley^{1*}, Colm Delaney^{2*}

¹ School of Physics and AMBER, SFI Centre for Advanced Materials and Bio-Engineering Research, Trinity
College Dublin, Dublin 2, Ireland.

E-mail: BRADLEL@tcd.ie

²School of Chemistry & AMBER, The SFI Centre for Advanced Materials
and BioEngineering Research, Trinity College Dublin, Dublin 2, Ireland.

E-mail: FLOREAL@tcd.ie; CDELANE5@tcd.ie

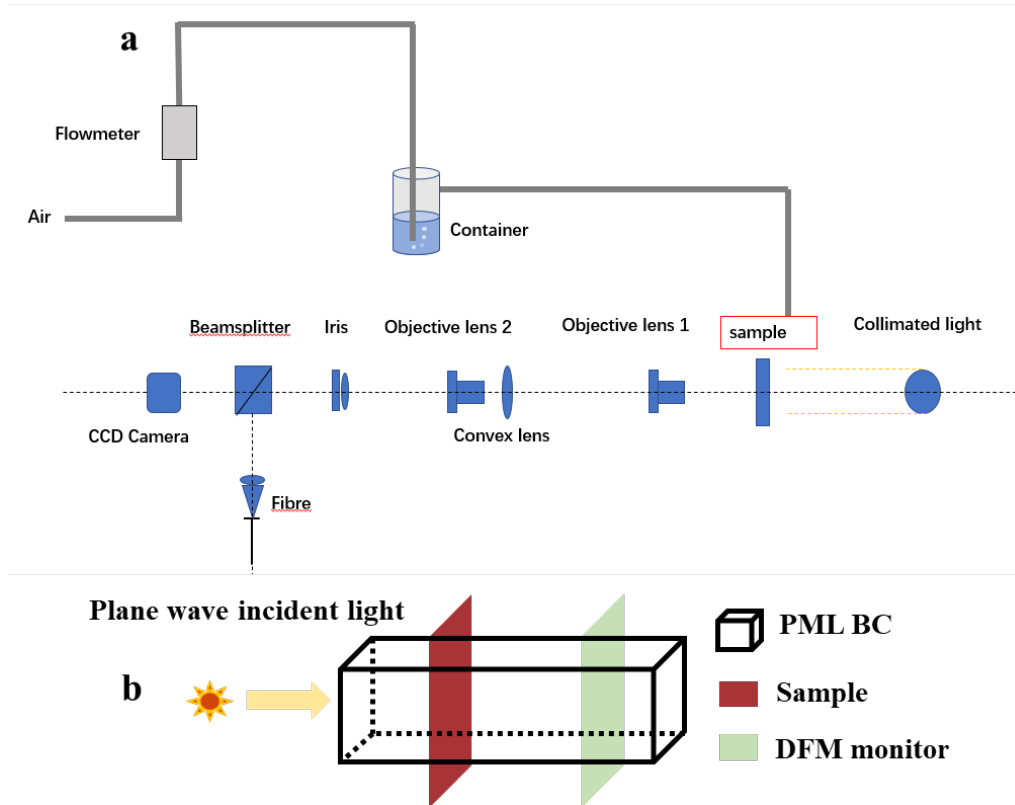


Figure S1. a) Home-built angle-resolved setup combined with a simple bubbling system. The sample is illuminated with an unpolarised collimated white light source. Specifically, a 5X and 20X objective lens (NA=0.12 and 0.4 respectively) was used in a home-built angle-resolved setup and a 4X objective lens (NA=0.1) was coupled with microscope for CCD image capture. b) Schematic shows the FDTD simulation settings.

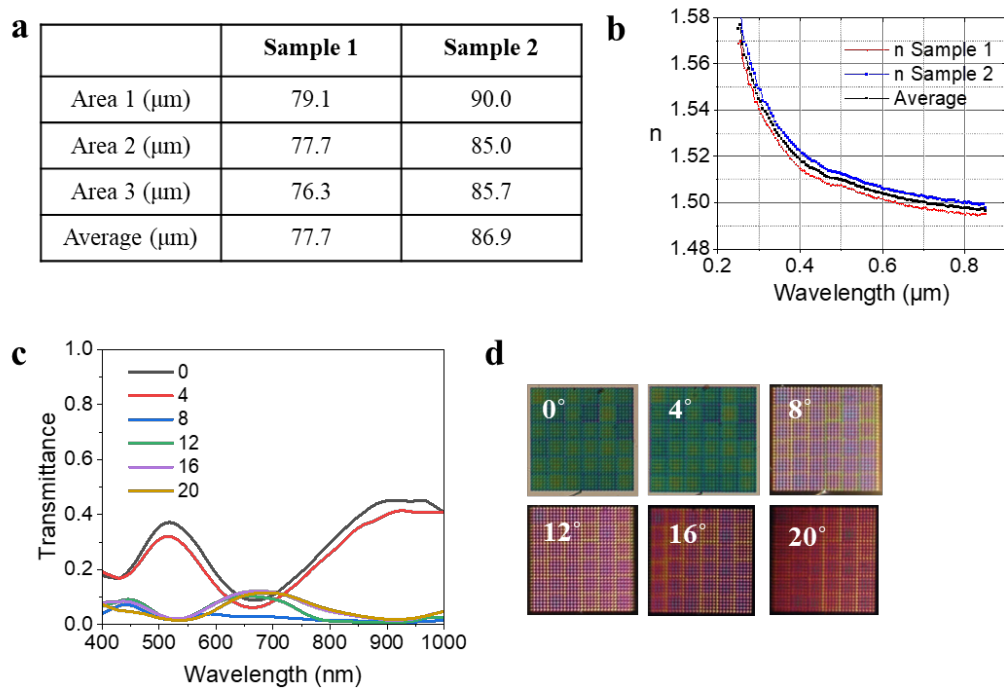


Figure S2. a) Film thicknesses of two hydrogel films measured using profilometer. b) Refractive indices of the films measured by spectroscopic ellipsometry. c) Angle dependent measurements of 11L spiral with designed structure dimensions of $d = 0.5 \mu\text{m}$, $s = 9.5 \mu\text{m}$, $g_1 = 2.0 \mu\text{m}$, $g_2 = 1.5 \mu\text{m}$, $g_3 = 2.5 \mu\text{m}$ and $h = 2.0 \mu\text{m}$. d) The corresponding structure color in Figure S2c.

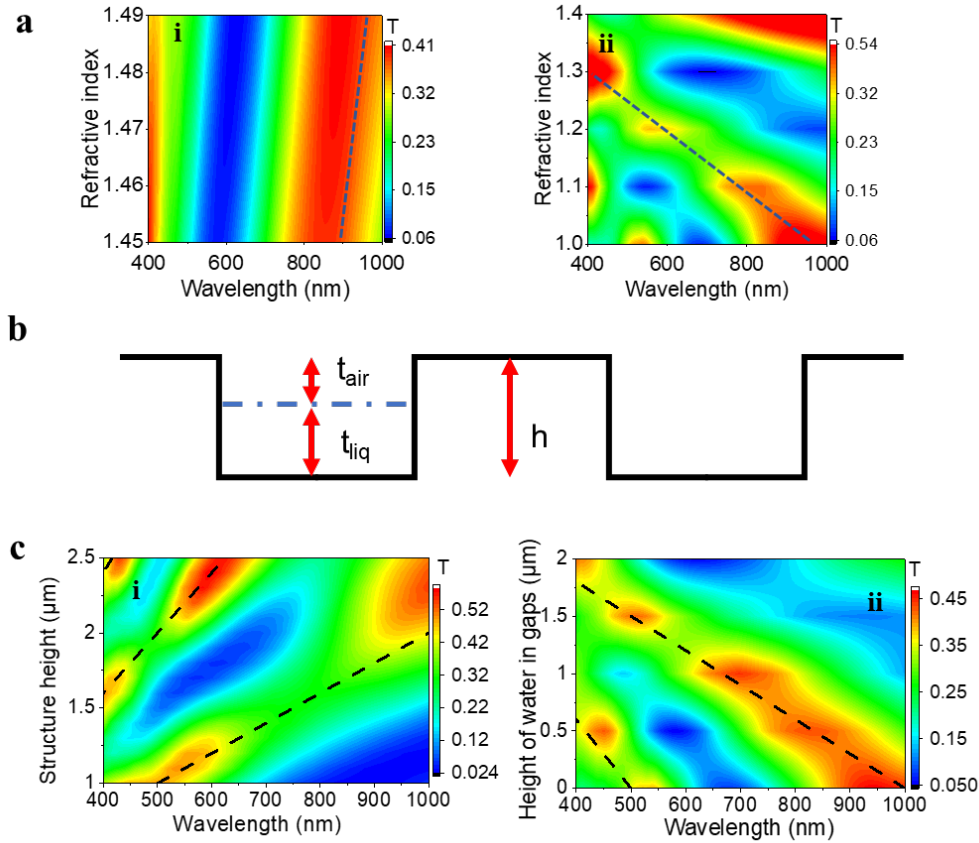


Figure S3. a) Contour maps of transmittance spectra from FDTD simulations show the trends as a function of the i) refractive index of the hydrogel and ii) refractive index of structure gaps. b) Schematic illustration of light passing through a grating, light will go through polymer with height of h and gaps which can be air or partially filled with a liquid (t_{air} and t_{liq} represent the gap height filled with air and liquid, respectively). c) Contour plot of simulated transmittance spectra of 11L concentric square spirals with i) varying structure height and ii) increasing height of water in gaps. The black dash lines represent the data calculated using $\lambda_0 = \{n_{\text{hydrogel}} \cdot h - [(n_{\text{liq}} \cdot t_{\text{liq}}) + (n_{\text{air}} \cdot t_{\text{air}})]\} / m$ where t_{air} and t_{liq} represent the gap height filled with air and liquid, respectively and $t_{\text{liq}} + t_{\text{air}} = h$ and m is the order. The above simulations are based on a structure model of $d = 0.9 \mu\text{m}$, $g_1 = 2.0 \mu\text{m}$, $g_2 = g_3 = 1.5 \mu\text{m}$, $s = 9.5 \mu\text{m}$.

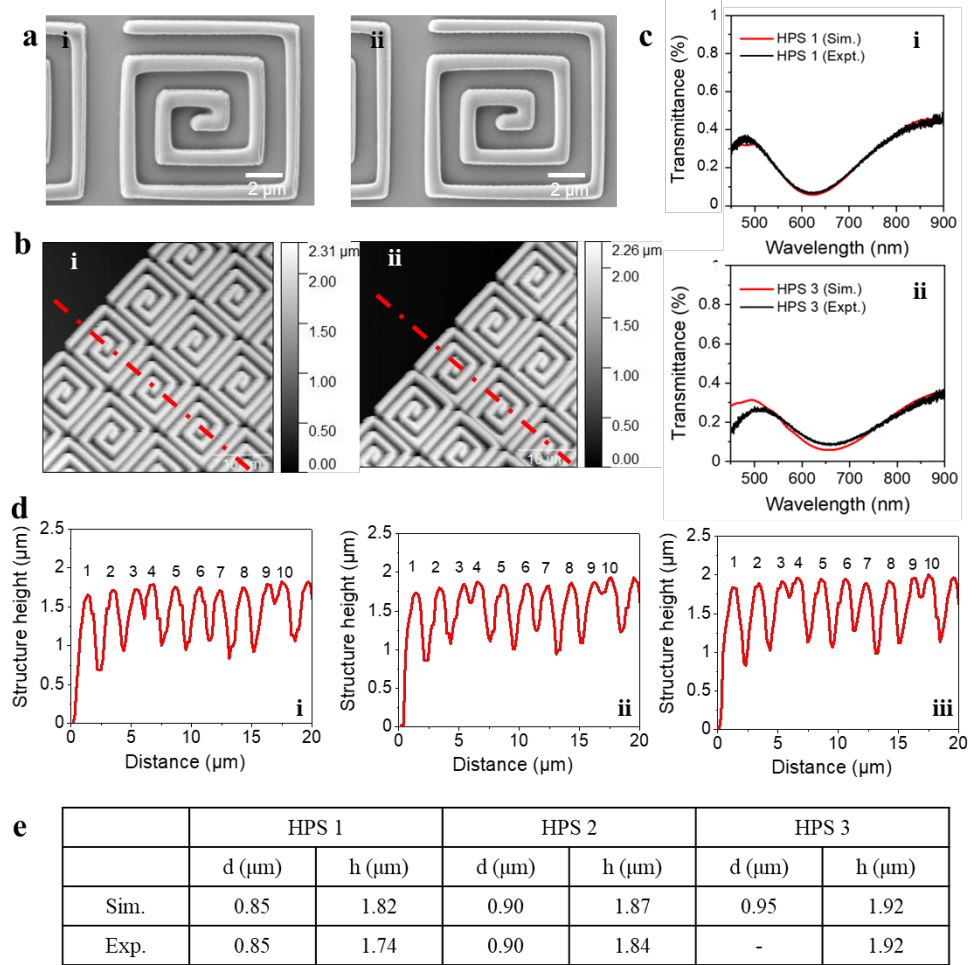


Figure S4. a) SEM images of HPS 1 and HPS 3 with designed dimensions of $g_1=2 \mu\text{m}$, $g_2=1.5 \mu\text{m}$, $g_3=1.5 \mu\text{m}$, $s=9.5 \mu\text{m}$ and $d=0.5 \mu\text{m}$, $h=1.0 \mu\text{m}$ fabricated using laser power of i) 25 mW, ii) 30 mW, respectively. b) AFM images of i) HPS 1 and ii) HPS 3. c) Comparisons of simulated and experimental zero-order transmittance spectra of i) HPS 1 and ii) HPS 3 in air. d) AFM height profiles of i) HPS 1, ii) HPS 2 and iii) HPS 3 corresponding to the red dashed lines in Figure S4b i), Figure 2b and Figure S4b ii), respectively. e) Table of simulation and experimental dimensions. The experimental values are an average of 10 measurements of SEM linewidth analysis and AFM height analysis.

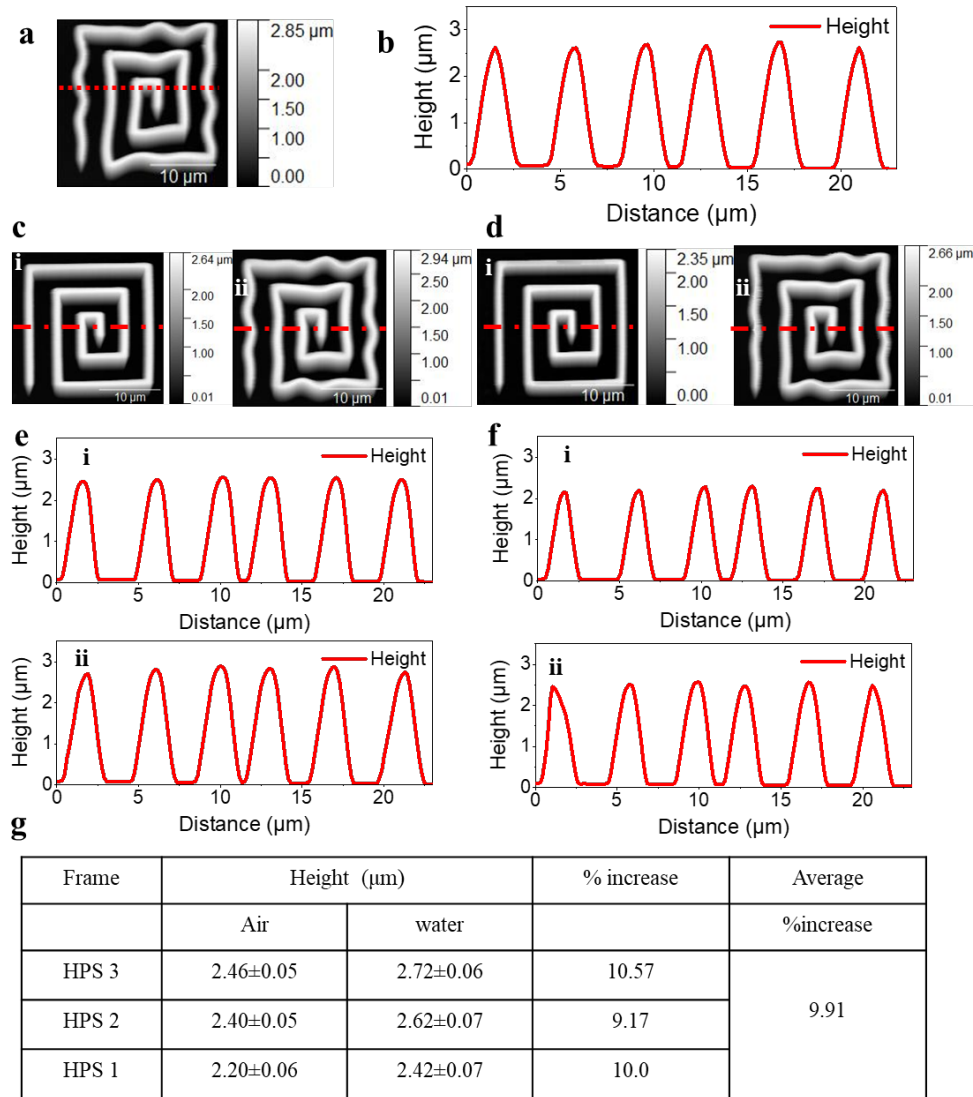


Figure S5. a) AFM image of an extended spiral immersed in water. The structure was fabricated using a laser power of 27.5 mW. b) Height analysis of the extended spiral immersed in water along red dashed line shown in a). c) and d) AFM images of extended spiral frames fabricated using 30 mW laser and 25mW laser power, respectively, i) in air and ii) immersed in water solution. e)(i) and f)(i) Two examples of the AFM height analysis of frame samples in c)(i) and d)(i), respectively, in air. e)(ii) and f)(ii) correspond to c)(ii) and d)(ii) where the samples are immersed in water. g) Average heights ($n=10$) using measurements along the vertical and horizontal axes.

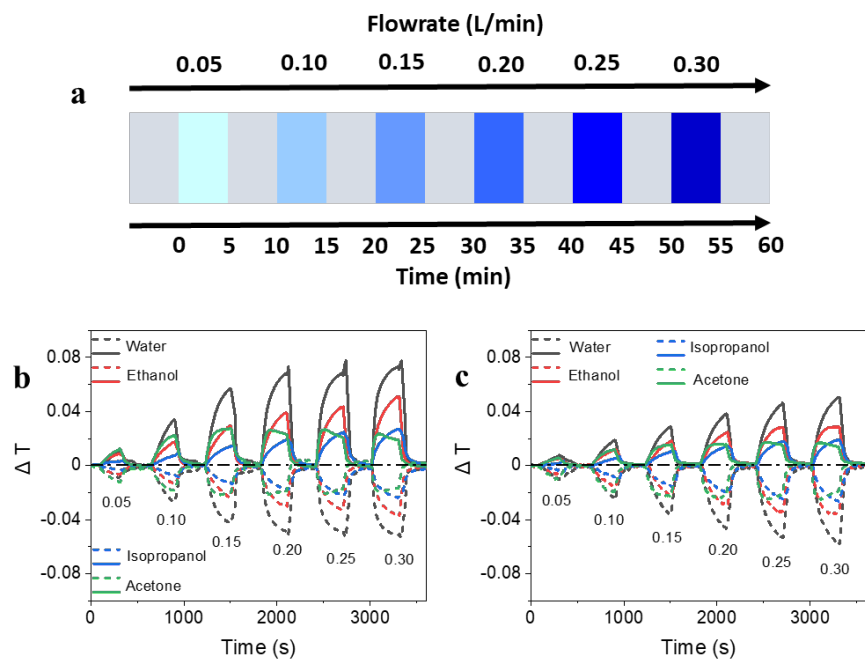


Figure S6. a) Schematic of the consecutive phases in the vapor responsive measurements. Grey areas represent the 5 minute drying process in dry air under a flowrate of 0.5 L/min. Blue areas correspond to the 5 minutes of vapor exposure at flowrates of 0.05 L/min to 0.3 L/min in 0.05 L/min increments. The whole process lasts 1 hour and 5 minutes. Change in transmittance (ΔT) of b) HPS 3 (30 mW laser power) and c) HPS 1 (25 mW laser power) as a function of exposure time at b) peak 516.9 nm (dotted line), trough 661.0 nm (solid line) and c) peak 482.8 nm (dotted line), trough 619.9 nm (solid line), respectively.

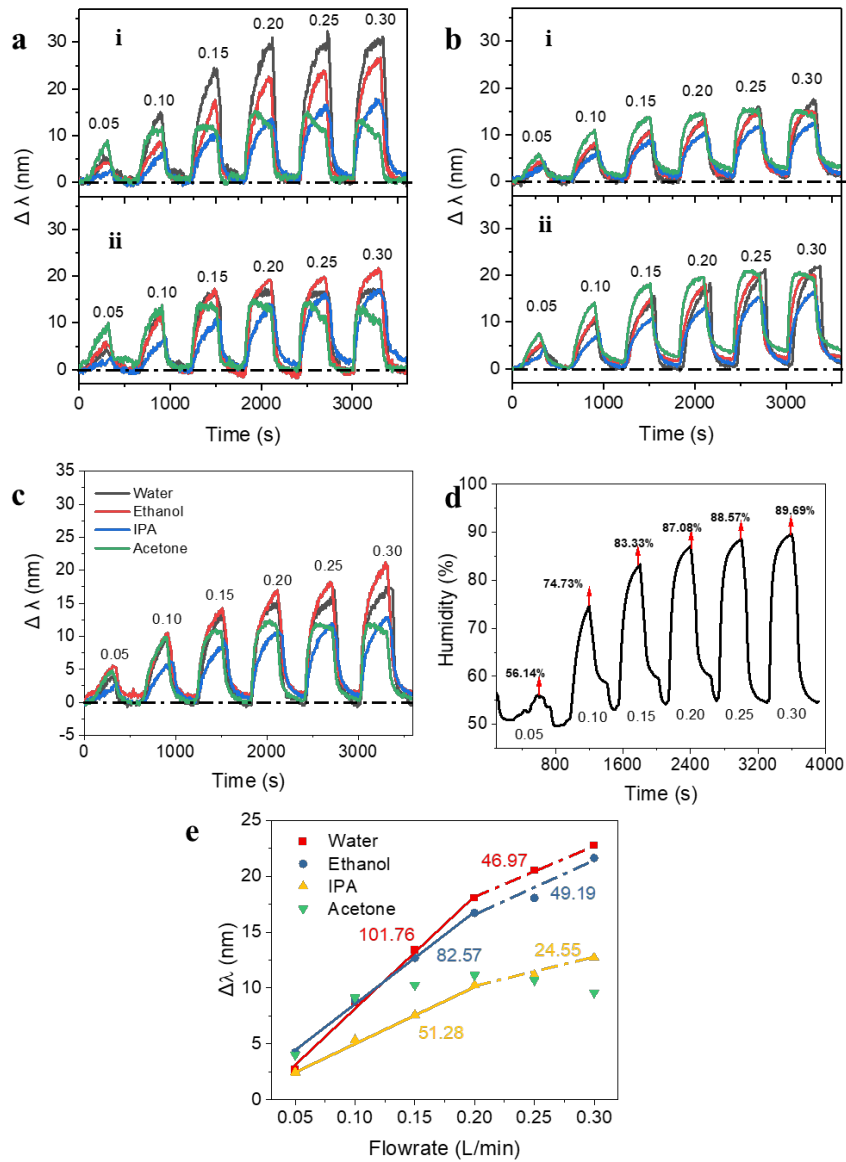


Figure S7. Change in wavelength ($\Delta\lambda$) of a) HPS 3 and b) HPS 1 at their i) peak and ii) trough wavelength, respectively. c) Delta wavelength ($\Delta\lambda$) of HPS 2 at the trough wavelength. d) Humidity measurements using a commercial sensor (TSP01, Thorlabs) by applying the process depicted in Figure S6a. e) $\Delta\lambda$ as a function of flowrate for HPS 2.

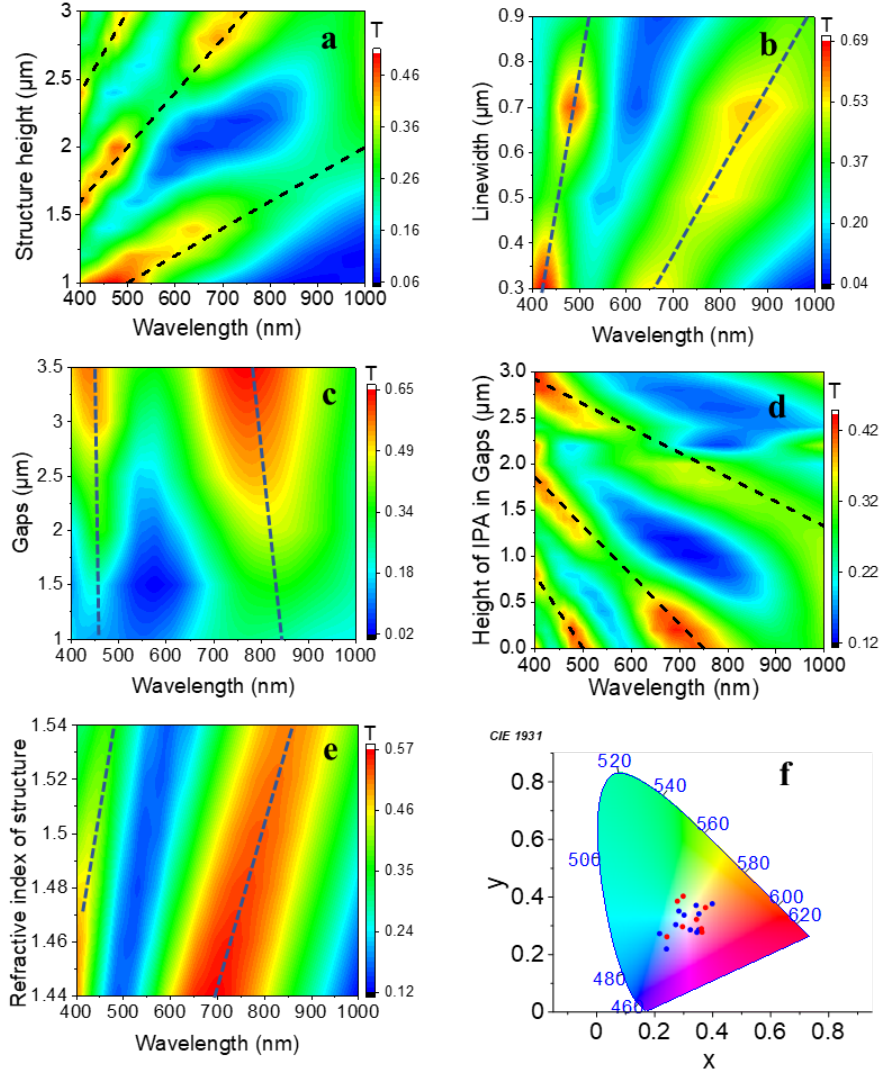


Figure S8. Contour maps of the FDTD simulation transmittance spectra of the 5L spirals as a function of a) structure height (with fixed parameters: $d = 1.1 \mu\text{m}$, $g_1 = g_2 = g_3 = 2.2 \mu\text{m}$), b) linewidth (with fixed parameters: $h = 2.0 \mu\text{m}$, $g_1 = g_2 = g_3 = 2.5 \mu\text{m}$), c) gaps between lines (with fixed parameters: $d=0.5 \mu\text{m}$, $h=2.0 \mu\text{m}$), d) height of IPA in gap (with fixed parameters: $d=1.1 \mu\text{m}$, $h=3.0 \mu\text{m}$, $g_1 = g_2 = g_3 = 2.2 \mu\text{m}$) and e) refractive index of material (with fixed parameters: $d=0.5 \mu\text{m}$, $h=2.0 \mu\text{m}$, $g_1 = g_2 = g_3 = 2.5 \mu\text{m}$). f) CIE 1931 chromaticity diagram shows the color coordinates of simulated pixels (blue dots) corresponding to a) and experimental pixels (red dots) in Figure 4d. The dash lines in Figure S8a and S8d are calculated using $\lambda_0 = (n_{\text{hydrogel}} - n_{\text{air}}) \cdot h/m$ and $\lambda_0 = \{n_{\text{hydrogel}} \cdot h - [(n_{\text{liq}} \cdot t_{\text{liq}}) + (n_{\text{air}} \cdot t_{\text{air}})]\}/m$, respectively.

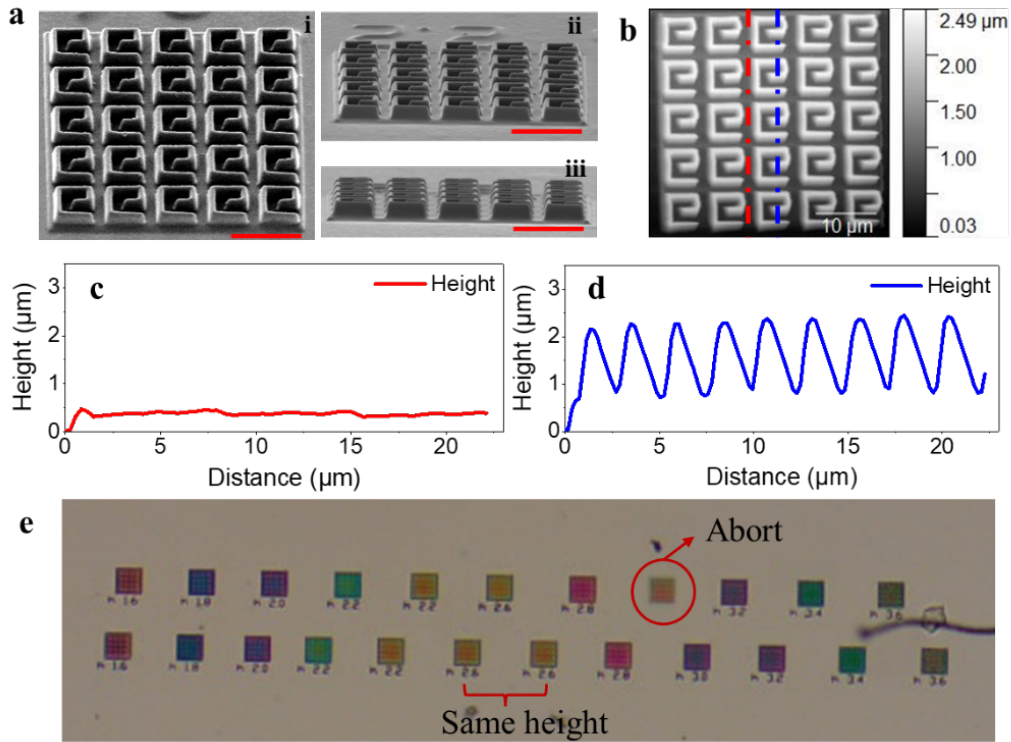


Figure S9. a) SEM images of the 5L spiral color pixel with $h=2.0\ \mu\text{m}$ in i) 45° tilted view, ii) 75° tilted view and iii) side-on. The red scale bar corresponds to $10\ \mu\text{m}$. b) An example of an AFM image of the 5L spiral with designed structure height of $1.0\ \mu\text{m}$ and underlying film height of $0.6\ \mu\text{m}$. c) An example of AFM height analysis of the bottom film, corresponding to the red dashed line trace in b). d) An example of AFM height analysis of this 5L spiral structure, corresponding to the blue dashed line trace in b). e) An array of structures over range of heights, corresponding to the color pixels in Figure 4b.

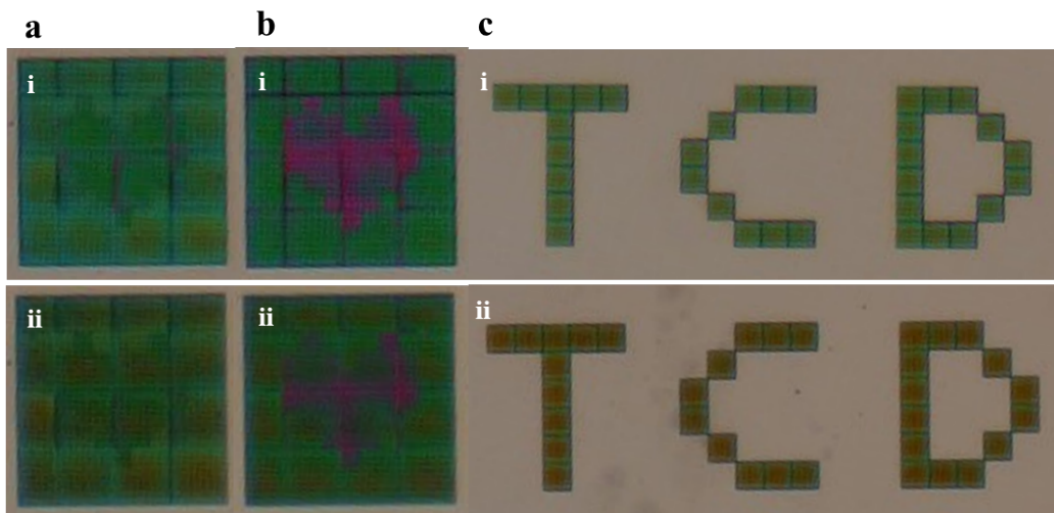


Figure S10. a), b) and c) CCD images of 3 patterns of 5L square spiral pixels in i) air and ii) water vapor. Water vapor here is produced by an ultrasonic humidifier. The images are collected using a 4X objective lens with NA=0.10.

Table S1. FDTD simulation heights and average experimental heights from AFM analysis of 5L spiral pixels with design heights from 1.0 μm to 3.0 μm . The average expansion limit in IPA calculated through AFM height analysis is also listed. The values are the average of n measurements.

$h_{\text{design}} (\mu\text{m})$	$h_{\text{sim}} (\mu\text{m})$	$d_{\text{sim}} (\mu\text{m})$	$h_{\text{AFM}} (\mu\text{m})$ in air (n=9)	$h_{\text{AFM}} (\mu\text{m})$ in IPA (n=9)	Expansion in IPA (n=6)
1.0	1.6	0.65	1.55	1.67	8%
1.2	1.6	0.65	1.82	1.97	
1.4	1.8	0.75	1.75	2.00	
1.6	2.1	0.8	2.09	2.23	
1.8	2.4	0.85	2.27	2.41	
2.0	2.4	0.85	2.39	2.50	
2.2	2.7	0.85	2.68	-	
2.4	3.0	0.9	2.83	-	
2.6	3.0	0.9	2.81	-	
2.8	3.2	0.95	2.87	-	
3.0	3.6	0.75	-	-	

Video S1. Optical microscopy transmission video of photonic QR code upon introduction of 2-propanol (real time).